BEAMFORMING BASED ON SPATIAL-WAVELET DECOMPOSITION

Wen Xu, Te-Chih Liu, and Henrik Schmidt

Ocean Acoustics Group
Massachusetts Institute of Technology
77 Mass. Ave, Room 5-204
Cambridge, MA 02139, USA
wenxu@mit.edu, tcliu@mit.edu

ABSTRACT

This paper presents a general framework for spatial wavelets processing in the context of a uniform linear array. By defining the scale in terms of the spatial sampling resolution, the spatial multi-resolution structure inherent in the array signal has an explicit representation based on the wavelet decomposition. Beamforming can then be implemented on the subband data. The new framework is applied to a real sonar target detection problem, and the traditional time-delay beamformer shows an improved computational efficiency. The efficiency gain is proportional to the number of sensors for targets near the broadside direction.

1. INTRODUCTION

Wavelets and filter banks are commonly used in time sampling signal processing. From the wavelet function, a set of orthonormal basis is generated by its translation and dilation, and a multi-resolution signal representation is then obtained by decomposing the given signal on this time-scale basis [1]. In the array problem, the data observations involve both temporal and spatial processes. At any time instant, the signal field (acoustic wave field, electromagnetic wave filed, etc.) is sampled at individual sensors, i.e., discrete space positions. At each sensor, the arriving signal is sampled at discrete time points. There exists essential similarity between the spatial-domain signal process and time-domain signal process: space sampling replacing time sampling and directional spectrum replacing frequency spectrum. It is thus quite natural to extend the concept of wavelets to the spatial aspect of array signal processing.

Most current array processing methods are implemented on the basis of a fixed, uniform spatial sampling regardless of signal source directions. This is not an optimum scheme for some source directions. Some research work has realized the advantages of the varying-sensor spacing scheme [2] [3]. Their basic idea is using several sensor pairs with different spacing. The pair with a small spacing (less than half a wavelength) is used to resolve the ambiguity, while the pair with a large spacing is used to obtain a high processing resolution. A multirate noise eigenvector processing is also developed in the context of the Beamspace Root-MUSIC implementation [4], but without involving the source direction and thus the spatial sampling resolution.

In this paper, a general framework for spatial wavelets processing is outlined in the context of a uniform linear array. This framework, first introduced in Ref. [5], perfectly describes the multi-resolution (sampling) structure inherent in the array signal. Beamforming can then be implemented on each subband of the wavelet decomposition. Advantages of the wavelet approach are demonstrated through examples of multi-sensor sonar imaging and target detection using both simulated and experimental data.

2. SPATIAL WAVELETS SCALE AND MULTIRATE SPATIAL SAMPLING

Wavelets techniques use the time-scale analysis instead of time-frequency analysis. For time sampling signal, the scale is defined based on the time sampling resolution. To apply wavelets to an array problem, one of the key issues is to understand the scale in an array signal.

A uniform linear array (ULA) with N point sensors is shown in Fig. 1. The spacing between two adjacent sensors is d. We assume that a plane wave propagates from direction θ with angular frequency ω, and that the signal field is fully coherent across the array. Thus the received signal at each sensor is just a delayed version with respect to the reference sensor. Ignoring the noise for the time being, the received signal at sensor n is

$$r_n = Ae^{j[\omega(t+\tau_n)+\varphi_0]}, \tag{1}$$

where A is the signal amplitude, φ_0 is the initial phase at the reference sensor, and τ_n is the propagation time delay from the reference sensor to sensor n. From the geometry shown in Fig. 1, it can be easily seen by choosing the first sensor as the reference sensor that $\tau_n = (n\text{-}1)d \sin\theta/c$ (c is

0-7803-7551-3/02/$17.00 ©2002 IEEE

the wave propagation speed in the medium). If we add the received signals from N sensors together, the total output is

$$r = Ae^{j[\omega t+\varphi_0]}\sum_{n=1}^{N} W_n e^{j(n-1)kd\sin\theta}, \qquad (2)$$

where $k=\omega/c$ is the wavenumber and W_n is the output weight.

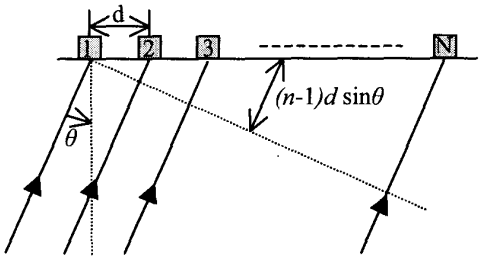

Figure 1: Configuration for a uniform linear array.

The summing term in (2) takes the exact form of a windowed discrete Fourier transform. Hence, we have a signal directional spectrum similar to the frequency spectrum for a time sampling signal. The frequency in a time signal spectrum corresponds to $kd\sin\theta$ in the space signal directional spectrum, which is a function of direction θ. Thus a spatial filter is to combine the outputs of the array sensors with complex gains and spatially filter the field such that a signal from a particular angle or set of angles is enhanced by a constructive combination and noise from other angles is rejected by destructive interference.

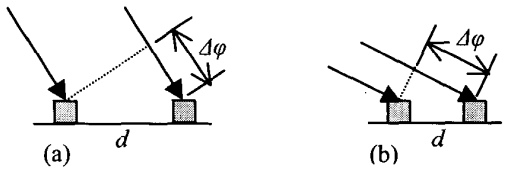

Figure 2: Spatial sampling spacings for the same phase difference observation between two adjacent sensors and different source directions: (a) near the broadside direction and (b) near the endfire direction.

It can be seen from (2) that the difference between the received signals at two adjacent sensors is contained in the phase term, $\Delta\varphi = kd\sin\theta$. Basically, this phase term determines the oscillation rate in a spatial signal. For a given sensor spacing, if a signal comes from near the broadside direction ($\theta \approx 0$), the phase term approximates zero. If a signal comes from near the endfire direction ($\theta \approx \pm\pi/2$), the phase term approximates $\pm kd$, the largest possible value. Accordingly, as shown in Fig. 2, for a source near the broadside direction, the signal oscillates slowly across the array, and we can observe it in a large scale, corresponding to large sensor spacing. In contrast, for a source near the endfire direction, the signal oscillates quickly across the array, and we have to observe it in a small scale, i.e., small sensor spacing. Therefore, the scale in a spatial signal is well defined based on the spatial sampling resolution.

This can be further understood from the spatial sampling criterion. To avoid phase ambiguity, a constraint is imposed on the phase difference between the received signals at two adjacent sensors:

$$|kd\sin\theta| = |\frac{2\pi}{\lambda}d\sin\theta| \le \pi, \qquad (3)$$

where λ is the wavelength. Then a spatial sampling criterion states

$$d \le \frac{\lambda}{2|\sin\theta|}. \qquad (4)$$

From (4), the spatial sampling interval depends on the signal direction. To satisfy this criterion for all physically resolvable directions within $(-\pi/2, \pi/2)$, the spacing between two adjacent sensors must not be larger than half a wavelength. However, for a direction component other than $\theta \approx \pi/2$, the sensor spacing can be larger, and a multirate spatial sampling technique is applicable.

As shown in Fig. 3, if we downsample a spatial signal by M, the corresponding sensor spacing increases to Md; if upsampling by M, the sensor spacing decreases to d/M. Many standard multirate processing techniques, for example the polyphase technique, can be applied to the implementation of spatial filters. Note that the sensor number is always finite, thus the spatial filter has a form of FIR filter.

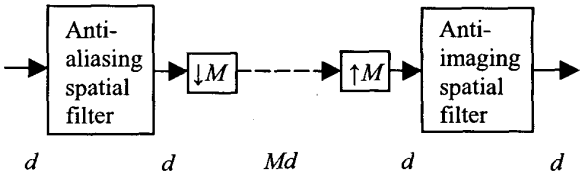

Figure 3: Downsampling and upsampling in spatial domain.

3. SPATIAL FILTER BANKS AND MULTI-RESOLUTION SIGNAL REPRESENTATION

Based on the above discussions, it is straightforward to apply the wavelet theory to array signal processing. Let s be a continuous space variable. The scaling function $\psi(s)$ and wavelet function $w(s)$ satisfy [1]

$$\text{Dilation equation: } \psi(s) = 2\sum_{k=0}^{K} H_L[k]\psi(2s-k) \qquad (5)$$

$$\text{Wavelet equation: } w(s) = 2\sum H_H[k]\psi(2s-k). \qquad (6)$$

$H_L[k]$ and $H_H[k]$ are the low-pass and high-pass spatial filter coefficients, respectively, and $H_L[0]+...+H_L[K] = 1$. The translation and dilation of the wavelet function

$$\{w_k^j(s)\} = \{2^{j/2} w(2^j s - k),\ k, j \text{ integer}\} \qquad (7)$$

form a set of orthogonal basis in spatial L^2 space. The scale level is set by j, and the normalized spatial sampling step at that level is 2^{-j}. Thus a spatial function, $x(s)$, can be analyzed and synthesized via the wavelet decomposition and reconstruction:

$$\text{Synthesis of a function: } x(s) = \sum_{j,k} b_k^j w_k^j(s), \qquad (8)$$

$$\text{Analysis of a function: } b_k^j = \int x(s) w_k^j(s) ds, \qquad (9)$$

where $\{b_k^j\}$ is the coefficient set of the wavelet decomposition at scale level j. Low-pass and high-pass filter bank can be used to implement the above procedure: anti-aliasing spatial filters and downsampling for analysis; upsampling and anti-imaging spatial filters for synthesis, as shown in Fig. 3. An example multi-level filter bank for the wavelet decomposition is shown in Fig. 4.

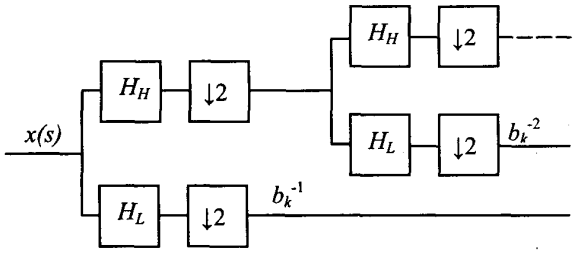

Figure 4: Filter bank for wavelet decomposition.

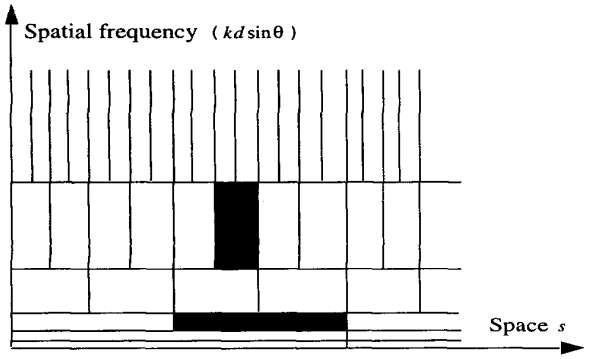

Figure 5: Space-spatial frequency resolution rectangles for wavelets. d is the fixed, real sensor spacing.

One has to be aware that because of the different underlying physics, the choice of the spatial filter differs from the time-sampled signal counterpart. For example, if a set of sources from continuous directions impinges on the array, a linear-phase filter is needed. This conflicts with the Orthogonality Condition [1] unless a Haar wavelet is used. In addition, design of the boundary filter and signal extension differs as well.

A multi-resolution structure is now valid for array signal representation, as shown in Fig. 5. The downsampling following the analysis filter changes the adjacent sensor spacing from $\lambda/2$ to λ and so on toward the coarser levels. Then the array signal is divided into different scales of spatial resolution (wavelet decomposition). From the filter point of view, a long spatial window is matched to a source near the broadside direction and a short spatial window is matched to a source near the endfire direction.

4. BEAMFORMING

4.1 True-Time Delay Bandpass Beamformer

As mentioned in Section 2, signals from individual sensors are combined to generate the array output. In order to steer an array in a particular direction, given the plane wave signal model, different time delays should be provided for different sensors so that signals coming from the desired looking direction are enhanced by coherent combination. A typical implementation is true-time delay bandpass beamformer [6] and three main processes are involved. First, the bandpass signal is demodulated to obtain its complex envelope, denoted by an in-phase component (I) and a quadrature component (Q). Second, each complex envelop is delayed accordingly based on signal time-delay τ_n. Finally, the complex envelope is rotated in phase. These procedures are usually realized using FIR interpolation filters. Fig. 6 gives the block diagram of this beamformer, where A/D is the analog-to-digital converter.

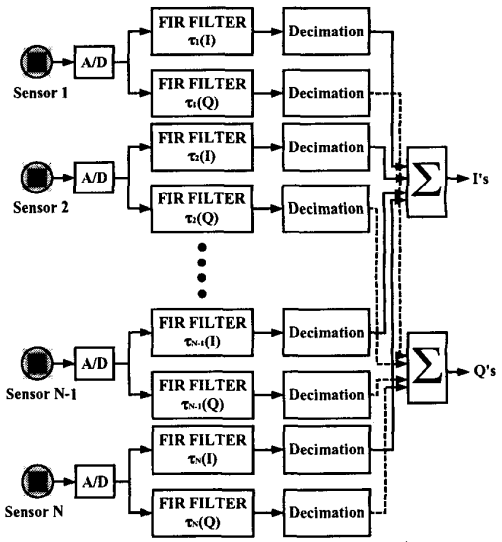

Figure 6: Block diagram of the time-delay beamformer.

4.2. Wavelet Approach

Recall that an array signal can be decomposed by applying the wavelet transform and that each subband samples the received signal field within corresponding angular intervals without ambiguity. It is thus natural to implement the beamforming on each subband of the wavelet decomposition. Fig. 7 describes such a modified beamformer operated on the first subband. Note that the wavelet operation in spatial domain does not change the operation in time domain.

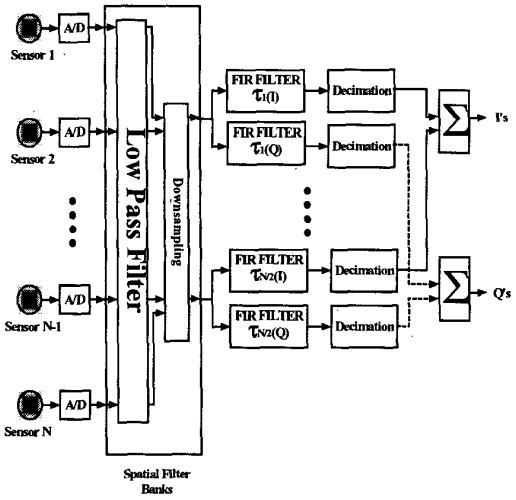

Figure 7: Block diagram of a modified time-delay beamformer with the wavelet decomposition.

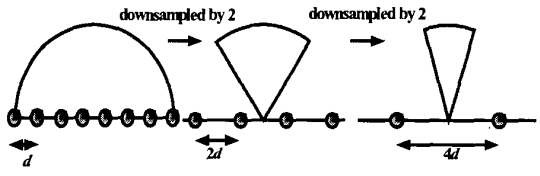

Figure 8: Illustration of the virtual sensor position and the corresponding resolvable region.

The wavelet transform can be efficiently realized using the filter bank shown in Fig. 4. Passing the signal into low pass/high pass filter and downsampling the output by 2, $2m$ signal channels at level j are reduced to m channels at level j-1, and the time delay for each channel is modified accordingly at each scale for the corresponding looking direction. In this multi-resolution scheme, as the array signals are broken into a coarser level in spatial domain, the corresponding resolvable region changes from $\pm\sin^{-1}(\pi/(2^{j}d))$ at level j to $\pm\sin^{-1}(\pi/(2^{(j-1)}d))$ at level j-1. The idea can be considered as moving the sensors into some virtual positions with the associated time delay and resolvable region, as illustrated in Fig. 8.

4.3 Advantages of the Wavelet Approach

At least two points make the wavelet scheme attractive. The first one is the computational efficiency. Using a multi-resolution signal representation, extra computational effort is required by the wavelet processing, but it is linearly proportional to the sensor number. In contrast, due to the reduced dimensionality of the subband data, the computational load for the beamforming operation is reduced significantly. For example, denote the sensor number N as 2^L, which can form L+1 subbands in space domain, N_s as the number of time-sampled points at each sensor, and N_f as the length of the interpolation filter in time domain. If the beam falls into subband j, j = 0, ..., -L, the wavelets approach reduces the computational load for beamforming processing by the amount of $(2^L - 2^{L+j}) \cdot N_s N_f$ multiplications while maintaining the same amount of additions. Fig. 9 shows an example of the computational efficiency at different subband levels of a 128-element ULA, which includes $N_s \cdot N$ additional filter bank operations. The computational load drops dramatically at level -6 in contrast to level 0 which corresponds to the original sampling step d. The benefit is more significant as the data sampling size increases.

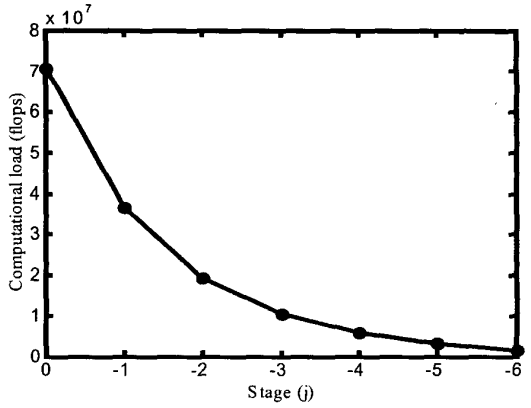

Figure 9: Comparison of the computational load at different subband stages. N_s=4096, N_f=128.

Second, direct processing of a subband automatically rejects noise and unwanted signals from other directional subbands, providing potentials for a better performance. This is illustrated in Fig. 10, in which the single-to-noise ratio at the beamformer output is computed at different subband stages using the simulated data under the same configurations in Fig. 9.

5. EXAMPLE

In this section, we apply the wavelet-based beamformer to perform the seabottom target detection. The sonar data are

taken from the GOATS (Generic Ocean Array Technology Sonar) 2000 experiment [7]. A uniform linear array of 8 omnidirectional elements is mounted on an autonomous underwater vehicle, collecting the acoustic data. The senor spacing is half a wavelength at frequency of 8 *KHz*. The wavelet decomposition using the Haar wavelet is first applied to the original sampled data. The beamformer processing is then implemented on each subband data for the corresponding looking direction with N_s = 4096 and N_f = 8. The beamformer forms a 9-beam image due to the resolution limitation of the physical array aperture. The resulting target images with and without the wavelet decomposition, respectively, are given in Fig. 11. A strong target is seen in both images. However, the two images are slightly different at each beam except the endfire one, which shows the suppression of spatial broadband ambient noise toward the lower stage subband using the wavelet approach. The computational load is reduced as well by the wavelet approach.

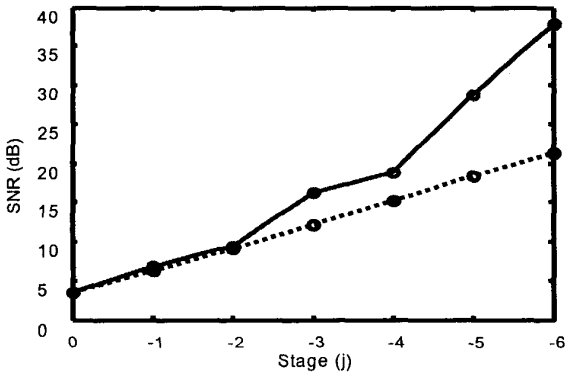

Figure 10: Comparison of the SNR at different subband stages. Solid line: with wavelet decomposition; dashed line: without wavelet decomposition.

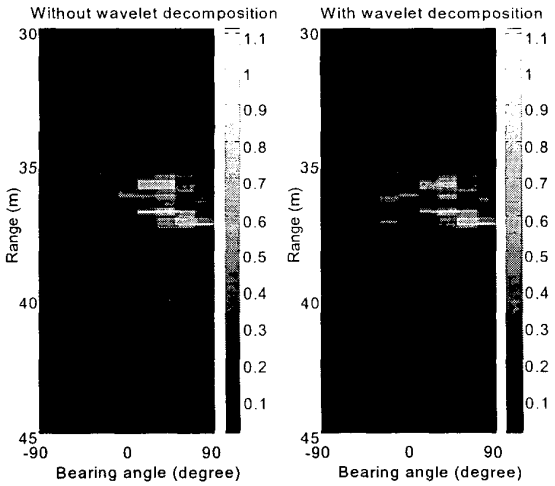

Figure 11: Example sea-bottom target images.

6. CONCLUSION

In this paper, wavelets and filter banks are applied to the array problem. Proceeding from a definition of the scale, a general framework for the application of wavelets to array signal processing is developed. Within this framework, the traditional time-delay beamformer can be implemented on data subbands available via the wavelet decomposition. Simulations and experimental data processing show improvements in performance over a standard approach. These improvements include better signal-to-noise ratio and reduced computational load. For the targets near the broadside direction, the efficiency gain in computation is proportional to the number of sensors. To generalize the wavelet approach to other beamformer methods such as the focused beamformer and to the case with broadband signal, many other issues need to be further investigated, for example, design of the wavelet filter.

7. REFERENCES

[1] G. Strang and T. Nguyen, *Wavelets and Filter Banks*. Wellesley, MA: Wellesley-Cambridge, 1997.

[2] M. D. Zoltowski and C. P. Mathews, "Real-time frequency and 2-D angle estimation with sub-Nyquist spatio-temporal sampling," *IEEE Trans. Signal Processing*, vol. 42, pp. 2781--2794, October 1994.

[3] A. N. Lemma, A. J. Van der Veen, and E. F. Deprettere, "Multiresolution ESPRIT algorithm," *IEEE Trans. Signal Processing*, vol. 47, pp. 1722--1726, June 1999.

[4] G. M. Kautz and M. D. Zoltowski, "Beamspace DOA estimation featuring multirate eigenvector processing," *IEEE Trans. Signal Processing*, vol. 44, pp. 1765--1778, July 1996.

[5] W. Xu and W. K. Stewart, "Multiresolution-signal direction-of-arrival estimation: A wavelets approach," *IEEE Signal Processing Letters*, vol. 7, pp. 66-68, March 2000.

[6] D. C. M. Horvat, J. S. Bird, M. M. Goulding, "True time-delay bandpass beamforming", *IEEE Journal of Oceanic Engineering*, vol. 17, pp. 185-192, April 1992.

[7] H. Schmidt and J. Edward, "GOATS: Multi-platform sonar concept for coastal mine countermeasures," In A. C. Schultz and L. E. Parker, editors, *Multi-Robot System: From Swarms to Intelligent Automata,* pp. 133-140. Kluwer Academic Publishers, 2002.